Green chemical synthesis for well-defined and sharply distributed SiO2@FexOy particles

Leis Florencia
CONICET: Consejo Nacional de Investigaciones Cientificas y Tecnicas
Long Leonel Andrés
CONICET: Consejo Nacional de Investigaciones Cientificas y Tecnicas
Di Virgilio Ana
CONICET: Consejo Nacional de Investigaciones Cientificas y Tecnicas
Pablo Arnal (arnal@quimica.unlp.edu.ar)
CONICET: Consejo Nacional de Investigaciones Cientificas y Tecnicas https://orcid.org/0000-0002-8252-7898

Research Article

Keywords: Core@shell particles, synthesis of nanostructured materials, iron oxide, silica, fluoride removal, green synthesis, cytotoxicity, genotoxicity

Posted Date: March 15th, 2021

DOI: https://doi.org/10.21203/rs.3.rs-248374/v1

Version of Record: A version of this preprint was published at Journal of Sol-Gel Science and Technology on April 1st, 2021. See the published version at https://doi.org/10.1007/s10971-021-05521-1.

Abstract

Using a non-toxic precursor, we created a green chemical synthesis for colloidal spheres with a core@shell structure having a silica core and an iron oxide shell (SiO_2@Fe_xO_y). Our synthesis pathway enabled an iron oxide shell formation with a 9 ± 6 nm thick shell onto colloidal silica spheres (ca. 700 nm). SiO_2@Fe_xO_y particles reduced A549 cell viability and induced DNA damage. SiO_2@Fe_xO_y particles showed the potential for removing fluoride from water.

Highlights

- Green chemical synthesis for monodisperse, spherical SiO_2@Fe_xO_y particles.
- A 9 ± 6 nm thick shell of iron oxide formed onto monodisperse silica spheres.
- The presence of the shell reduced A549 cell viability and induced DNA damage.
- SiO_2@Fe_xO_y particles removed fluoride from water in batch systems.

1. Introduction

The necessity to reduce fluoride concentration in water has inspired many researchers worldwide to investigate different potential solutions scientifically. Among them are the processes involving solid materials with sufficient affinity for pollutants to reduce their water concentration down to harmless values [1, 2].

Colloidal particles with a core of silica (SiO_2), a shell of another oxide (M_xO_y), and a sharp distribution in size centered at 100—1000 nm (from now on SiO_2@M_xO_y for the sake of simplicity) combine several valuable attributes regarding removing pollutants from water. The synthesis of monodisperse silica particles is available in the scientific literature since the pioneering work of Stöber *et al.* [3]. Metal oxides have a high concentration of active functional groups on their surface, capable of removing pollutants from water [4]. Mesoporous shells (pores 2–50 nm) provide high surface areas (> 100 $m^2.g^{-1}$) without the high toxicity of nanoparticles with similar surface areas and without the difficulties of recovering nanoparticles from solution. Spherical particles with a sharp distribution in size offer the least possible resistance to the pollutant's flow from the bulk solution towards their outer surface, mainly when spherical particle agglomerate (form more giant clusters).

Iron oxide has a well-known affinity for fluoride present in water [5, 6]. Hence, SiO_2@Fe_xO_y are potentially valuable materials for fluoride decontamination. In contrast with particles with an iron oxide core covered with silica [7–13], the synthesis of SiO_2@Fe_xO_y is a rarity in the scientific literature. A synthesis protocol for SiO_2@Fe_xO_y particles is available [14]. However, that synthesis protocol uses an iron precursor (iron acetylacetonate) with acute oral toxicity (see, for instance [15]). Besides, no information is available regarding SiO_2@Fe_xO_y's cyto- and genotoxicity and its ability to remove fluoride from water.

This work's main aims were (a) to develop a less polluting and dangerous synthesis (a green chemical synthesis [16]) for SiO_2@Fe_xO_y particles, (b) to explore their cyto- and genotoxicity, and (c) to test their potential ability to remove fluoride from water. Our primary hypothesis was that $Fe(NO_3)_3.9H_2O$ (that lacks the toxicity of iron acetylacetonate [17]) would form nanometer-thick shells on silica spheres dispersed in ethanol. An additional hypothesis in this work was that the presence of an iron oxide shell would enhance cyto and genotoxic effects on alveolar epithelial lung cells in culture. The last hypothesis of this work was that SiO_2@Fe_xO_y would remove fluoride from water.

2. Materials And Methods

2.1 Synthesis of SiO_2@Fe_xO_y

SiO_2@Fe_xO_y particles were synthesized in a two-step process. In step 1, monodisperse silica spheres were synthesized following a sol-gel process previously reported [18]. Shortly, 4.2 mL of tetraethyl orthosilicate (TEOS) were injected (one-way 10 mL syringe with metallic needle) through a septum into a solution of 22 mL NH_3 in H_2O (30% w/w) and 64 g of absolute ethanol. This solution contained in a 500 mL round bottom flask with one neck was previously warmed up in water at 33°C. One hour after injecting TEOS, the white solid particles were separated from the solution (centrifugation at 5000 rpm for 5 min). Then, particles were washed by dispersing in 100 mL of distilled water and separating the liquid (centrifugation at 5000 rpm for 5 min) three times. Afterwards, particles were washed three times using a similar procedure, but using absolute ethanol instead of water. Finally, the solid particles were dispersed in 100 mL of absolute ethanol.

In step 2, a solution of 0.14 g of $Fe(NO_3)_3.9H_2O$ in 10.00 mL of absolute ethanol was added drop-wise from a burete a to the dispersion of silica spheres in a 500 mL round flask with one neck under magnetic stirring. Previously, the flask with the dispersion was allowed to warm up in water at 33°C (closed with a septum). After addition of the iron precursor, the flask remained closed under stirring overnight. The originally white dispersion turned yellow (**Scheme 1**). Finally, the solid particles were separated from the solution (centrifugation at 5000 rpm for 4 min) and dried at 60°C overnight

2.2 Characterization of Materials

Scanning Electron Microscopy (SEM). SEM images were obtained for silica and SiO_2@Fe_xO_y particles after covering with ca. 10 nm gold. Measurements were performed with a microscope JEOL JCM-6000 Neo Scope. To determine particle size distribution, the diameter of 96 silica particles and 66

SiO_2@Fe_xO_y particles were measured. A detailed description of the procedure is in the supplementary information. Thickness of shells was estimated by subtracting the mean diameter of particles after and before addition of the iron precursor.

Energy-dispersive X-ray Spectroscopy (EDX). Presence of oxygen, silicon, and iron and their distribution in particles was estimated with EDX. Measurements were performed with a microscope JEOL JCM-6000 Neo Scope.

Thermal Gravimetric Analysis Differential Thermal Analysis (ATG-DTA). ATG-DTA were performed with the equipment TG-DTA and TMA Rigaku Evo plus II either under air or N_2 from room temperature up to 1000°C at 10°C.min^{-1}.

X-Ray Diffraction (XRD). The diffractogram from the material after the synthesis was obtained in reflexion mode with the x-ray diffractometer Philips PW-3710.

Removal of Fluoride in batch systems. The removal of fluoride in batch systems with SiO_2@Fe_xO_y was studied with 2^2 factorial design [19]. Studied factors were solid-to-liquid ratio (S/L) and time after forming the batch system. Levels were 1 and 10 $g.L^{-1}$ in the former and 30 and 120 min in the latter. The fluoride concentration in an aqueous solution was measured with a selective fluoride ion electrode (VAN LONDON-PHOENIX) according to [20]. For each measurement, a sample was taken from the batch system, and it was centrifuged at 1500 rpm for 15 min. The supernatant was then separated and diluted 1:1 with TISAB buffer. Finally, the electrode was immersed in that solution while stirring, and the reading was taken in mV. The concentrations in milligrams per liter were obtained from the calibration curve data as indicated by the method.

Cyto- & Genotoxicity of SiO_2@Fe_xO_y particles

Cell culture. The A549 human lung carcinoma cell line was cultured in DMEM supplemented with 10% FBS, 100 U/mL penicillin, and 100 µg/mL streptomycin at 37°C in a humidified atmosphere with 5% of CO_2. Cells were seeded in a T75 flask, and when 80–90% of confluence was reached, cells were subcultured using TrypLE™. Experiments were carried out in multiwell plates, where cells were allowed to attach and were washed with DMEM before each treatment.

Cell viability assay. Monolayer cell viability was determined using 3-(4,5-dimethylthiazol-2-yl)-2,5-diphenyltetrazolium bromide (MTT), which is reduced by mitochondria in viable cells to a purple formazan dye [1]. Briefly, 2.5 x 10^4 cells were seeded on 96-well plates and incubated at 37°C. After 24 h, cells were exposed to different suspensions of each particle for 24 h. Afterward, the monolayers were washed and incubated with 0.5 mg/mL of MTT in DMEM for 3 hours. The absorbance of the formazan extracted with DMSO (100 µL/well) was recorded at a wavelength of 570 nm by using a multiplate reader Multiskan FC (Thermo Scientific). The cell viability is shown graphically as a percent of the control value.

Genotoxicity study. For detection of DNA damage, the single cell gel electrophoresis assay (Comet assay) was employed based on the method of Singh et al. [2] with minor modifications. Briefly, A549 cells were treated with different suspensions of the particles. After 24 h, cells were suspended in 0.5 % low melting point agarose and immediately poured onto microscope slides precoated with 0.5 % normal melting point agarose. Two slides were prepared for each condition; one slide was used to observe double and single-stranded DNA breaks and the other was used to obtain information on the presence of oxidized DNA bases using digestion with the enzyme EndoIII [3]. Slides were immersed in ice-cold lysis solution (2.5 M NaCl, 100 mM Na2-EDTA, 10 mM Tris–HCl, 1% Triton X-100, 10% DMSO at 4°C, pH 10) for 1 h to lyse the cells, remove cellular proteins and to allow DNA unfolding. After that, the slides were washed three times with enzyme buffer (0.1 M KCl, 0.5 mM Na2-EDTA, 40 mM HEPES–KOH, 0.2 mg/ml bovine serum albumin (BSA), pH 8.0) and incubated for 45 min at 37°C with EndoIII in the enzyme buffer or with buffer alone. Then, the slides were placed on a horizontal gel electrophoresis tank, and the DNA was allowed to unwind for 20 min in freshly prepared alkaline electrophoresis buffer (300 mM NaOH and 1 mM Na2-EDTA, pH 12.7). Electrophoresis was carried out in the same buffer for 30 min at 25 V (≈ 0.8 V/cm across the gels and ≈ 300 mA) in an ice bath condition. Afterward, slides were neutralized and stained with SYBR Green. The analysis was performed in an Olympus BX50 fluorescence microscope. A total of 150 randomly captured cells per experimental point were used to determine the Tail Moment using Comet Score version 1.5 software. A pulse of 20 min of 10 µg/mL bleomycin just before the cells were harvested was employed as the positive control.

2.3 Statistical analysis

Three independent synthesis of SiO_2@Fe_xO_y were performed. All three samples were mixed into one batch. All experiments were performed with this mixture.

In estimating mean particle size and shell thickness, we use the Student's t-test with unknown but equal variances (pp337-344 [21]). To corroborate the equality of variances we carried out a quantitative hypothesis test using the F distribution ($\alpha = 0.05$) (pp355-359 [21]). The result of the layer thickness was expressed as the mean difference between the particles before and after shell formation ± the 95% confidence interval on the difference in means (pp345-347 [21]) (LCL and UCL for lower and upper confidence limit of the interval). To perform the t-test it is necessary that the distributions under study are normal. For this, a qualitative normality test was carried out using Q-Q plot graphs (pp212-251 [21]) and a quantitative normality test using the modified Shapiro-Wilks normality test [22] ($\alpha = 0.05$). Both tests were performed with INFOSTAT software [23]. Faced with the evidence of the absence of normality of the data, the presence of anomalous data (outliers) within each distribution was confirmed by means of the Q-Q plot. Therefore, the Grubbs test [24] for the detection of anomalous values ($\alpha = 0.05$) was used. This test detects one outlier at a time. This outlier is removed from the data set and the test is repeated until no outliers are detected. This procedure was performed in OriginPro 2016 software. Once the distributions without outliers were obtained, it was confirmed whether they are normal with the same methods described above. From these distributions, the statistically significant

difference between the areas of the particles obtained in step 1 and 2 of Sect. 2.1 (determination of layer thinness) was determined by means of the t-test. This test was carried out in INFOSTAT.

In fluoride removal, statistical analysis of the data was carried out by ANOVA (pp472-479 [21]), followed by the Fisher' Least Significant Difference (LSD) (p497 [21]) ($\alpha = 0.05$) procedure to discriminate among the means using INFOSTAT software.

In cyto- and genotoxicity studies, statistical analysis of the data was carried out by ANOVA, followed by the Fisher' Least Significant Difference (LSD) procedure to discriminate among the means. Results were expressed as the mean of three independent experiments and plotted as mean ± standard error of the mean. The total number of repeats (n) is specified in the legends of the figures. Analysis of the data was performed with STATGRAPHICS Centurion XVI.I.

3. Results

3.1 $SiO_2@Fe_xO_y$ formed with our synthesis

Our synthesis covered spherical silica particles with a sharp distribution in size with a homogeneously thick, nm-sized layer of an iron-oxide shell ($SiO_2@Fe_xO_y$). Evidence supporting this claim follows on.

First, particles kept their spherical shape after the synthesis (**Figure 1**). After the synthesis, only spherical particles were present. The addition of $Fe(NO_3)_3{\cdot}9H_2O$ dissolved in absolute ethanol did not form irregularly shaped particles. If they had formed, those iron oxide particles would be visible among the spheres. They are not. Also, spherical particles significantly increased their mean diameter. The shell formed during the synthesis has a mean thickness of 9 ± 6 nm.

Second, silica particles originally white became yellow after the synthesis (see **Figure 10** in SI). Before the synthesis, the solid showed the typical white color of silica spheres. After the synthesis, the solid showed the typical yellow-brown color of iron oxide.

Third, the yellow-brown particles obtained after adding iron nitrate contained significant amounts of iron. They contained 5% of iron that homogeneously distributed among spherical particles according to EDX analysis (see **Figure 12** in SI).

Finally, additional evidence supporting iron oxide's presence onto silica particles came from a thermal gravimetric and differential thermal analysis. After exposure to iron nitrate, particles experienced a mass loss at ca. 200 °C that was absent in silica spheres (**Figure 2**). The mass loss at ca. 200 °C corresponded to an exothermic process (**Figure 3**). X ray diffraction (see **Figure 11** SI) showed that crystalline phases were absent in as synthetized particles. The exothermic process at 200 °C likely correspond to the crystallization of the iron oxide at the shell.

All in all, all evidence shows that $SiO_2@Fe_xO_y$ formed successfully in our synthesis. So, we continued testing the $SiO_2@Fe_xO_y$ particle's ability to remove fluoride from water.

3.2 $SiO_2@Fe_xO_y$ remove fluoride from water

After exposure to iron nitrate that enabled the formation of $SiO_2@Fe_xO_y$ particles, fluoride removal significantly increased. In batch systems with S/L 10 $g.L^{-1}$, $SiO_2@Fe_xO_y$ particles successfully removed fluoride from water in less than 30 min. Fluoride significantly dropped its concentration from 42 to 16 ppm in less than 30 min (LSD Fischer, $p < 0.05$). The removal capacity was 2.4 $mg.g^{-1}$. Times of removal 30 and 120 min did not show a significant change in concentration (LSD Fischer, $p > 0.05$). In batch systems with S/L 1 $g.L^{-1}$, $SiO_2@Fe_xO_y$ particles did also significantly remove fluoride from water. Fluoride dropped its concentration from 42 to 39 ppm (LSD Fischer, $p > 0.05$). A detailed presentation of the data and calculations performed is at the SI. Summing up, the successful fluoride removal from water in batch systems in less than 30 min supports $SiO_2@Fe_xO_y$ particles' formation.

3.3 Cyto- and Genotoxicity of $SiO_2@Fe_xO_y$

The change in the particles' cyto- and genotoxicity after exposure to iron nitrate supports the formation of $SiO_2@Fe_xO_y$.

Exposure to iron nitrate changed the spherical particle's cytotoxicity. Exposing A549 cells to dispersions of either SiO_2 or $SiO_2@Fe_xO_y$ showed a statistically significant decrease of around 20% in cell viability from 0.05 $g.L^{-1}$ SiO_2 and 0.1 $g.L^{-1}$ $SiO_2@Fe_xO_y$ (**Figure 4**). However, with 1 $g.L^{-1}$ $SiO_2@Fe_xO_y$, cell viability significantly worsened, inducing an effect of 50% ($p < 0.001$, $n = 12$) (**Figure 4**).

Exposure to iron nitrate changed the spherical particle's genotoxicity. $SiO_2@Fe_xO_y$ particles were unable to significantly cut DNA strands in A549 cells (comet assay) (**Figure 5**). However, $SiO_2@Fe_xO_y$ particles significantly oxidized pyridinic DNA bases in A549 cells (comet assay with Endo III).

4. Discussion

We found that our synthesis with a non-toxic iron precursor enabled the formation of a nanometer-thick layer of iron oxide onto silica spheres. $SiO_2@Fe_xO_y$ particles successfully formed. This finding rests on evidence brought by three primary experimental sources: (a) Physico-chemical analysis, (b) cyto- and genotoxicity studies, and (c) fluoride removal in batch experiments. After exposure to iron nitrate, each particle had a core@shell structure

with a silica core and an iron oxide shell. The iron oxide shell was nanometer-thick and likely crystallized upon thermal treatment at ca. 200°C. After exposure to iron nitrate, cyto- and genotoxicity of particles significantly increased. The toxicity increment happened because of the presence of the iron oxide shell. After exposure to iron nitrate, particles significantly increased their ability to remove fluoride from water. Batch experiments showed the potentiality of $SiO_2@Fe_xO_y$ particles in removing fluoride from water indicating the presence of the iron oxide shell.

The synthesis of $SiO_2@Fe_xO_y$ particles is rare in the scientific literature. Meng *et al*. proposed a synthesis pathway starting from iron acetylacetonate [14]. Though the shell's formation mechanism is unknown, it likely involved a sol-gel process. In a sol-gel process, a nanometer-thick shell would form onto silica spheres following a complex combination of hydrolysis and condensation elementary reactions [25]. Inspired by that sol-gel processes, metal nitrates' ability to form well-defined films [11], and that iron(III) nitrate-nonahydrate forms solutions in ethanol [26], we proposed a new synthetic pathway for $SiO_2@Fe_xO_y$. Using iron(III) nitrate-nonahydrate eliminates the troubles generated by the toxicity of iron acetylacetonate. Also, we assumed that restricting the amount of water to that provided by the iron precursor would favor forming a homogenous shell onto silica spheres and avoid secondary nucleation. Secondary nucleation would lead to the unwanted formation of iron oxide particles. Our hypothesis found experimental support in this work. This work's synthesis pathway produces $SiO_2@Fe_xO_y$ particles.

$SiO_2@Fe_xO_y$ particles' cyto- and genotoxicity studies served a twofold purpose. First, the change in particles' toxicity supports the formation of an iron oxide shell. The material at the surface of the particle defines its chemistry. According to scientific literature, colloidal particles with iron oxide surfaces are more toxic than silica surfaces [27]. Second, our work offers the first information about the toxicity of $SiO_2@Fe_xO_y$ particles. This preliminary information is relevant, considering the potential use of $SiO_2@Fe_xO_y$ particles in removing pollutants from water. The toxicity of material for water filtration is relevant, especially when part of the material —for instance, colloidal particles— may unwantedly find their way into filtered water. Our study shows that the iron oxide shell's presence altered lung epithelial cells' cell viability and induced oxidative DNA damage in the concentration range of 0.1-1 mg/mL. These findings have coherence since iron oxide's previous results produce cytotoxicity *in vitro* [28][29]. However, the concentrations used in this study were much higher than the concentration range of silica particles in working places which turned out to be $0.04\ x10^{-6}$ – $5x10^{-6}$ [30]. This outcome allows us to ensure a margin of safety in occupational settings.

$SiO_2@Fe_xO_y$ particles' fluoride removal studies served a twofold purpose, too. First, the ability to remove fluoride supports the formation of an iron oxide shell. The scientific literature indicates that silica has a low affinity to fluoride [31]. In contrast, iron oxide has a high affinity for fluoride [5, 6]. Second, this study provides promising information about $SiO_2@Fe_xO_y$ particles' ability to remove fluoride. Equilibration times in batch systems lower than 30 min and removal capacities of 2.4 $mg.g^{-1}$ places $SiO_2@Fe_xO_y$ particles among top performers in fluoride removal [32–34].

Our experiments show that $SiO_2@Fe_xO_y$ particles formed successfully and stand out as potential candidates to remove fluoride from water. However, our study has some limitations. This study does not provide the exact composition nor a characterization of the shell's structure. Nor does this study show the full potential of $SiO_2@Fe_xO_y$ particles' ability to remove fluoride.

We endorse future studies with $SiO_2@Fe_xO_y$ particles. Knowledge about the formation mechanism, the structure, and the chemistry of the shell shall provide a solid understanding of the synthesis and potentiality of $SiO_2@Fe_xO_y$ particles. Formation of iron oxide shells with high surface area —as already obtained for zirconium and titanium oxide [18, 35]— shall improve $SiO_2@Fe_xO_y$ particles' capacity to remove fluoride from water. Moreover, because of iron oxide's affinity for other anionic pollutants of water like arsenate, $SiO_2@Fe_xO_y$ particles might become an excellent material to remove anions from water in general.

5. Conclusion

In conclusion, our data proved that $SiO_2@Fe_xO_y$ particles formed successfully when an ethanol solution of iron(III) nitrate-nonahydrate dripped into a dispersion of silica spheres in ethanol under stirring. The new synthesis pathway proposed in this work shows that it is possible to prepare $SiO_2@Fe_xO_y$ particles without using acutely toxic materials, as previously reported. With an iron oxide shell 9 ± 6 nm thick, $SiO_2@Fe_xO_y$ particles showed a somewhat higher cyto- and genotoxicity than bare silica spheres. $SiO_2@Fe_xO_y$ particles also showed their potential in removing fluoride from water.

Declarations

Acknowledgments

CONICET (PIP-2013-0105, Leonel Long's doctoral fellowship), ANPCYT (PICT-2014-2583 & PICT 2016-0508), and UNLP (PPID 2018) partially supported this study.

Funding

Consejo Nacional de Investigaciones Científicas y Técnicas (PIP-2013-0105, Leonel Long's doctoral fellowship), Agencia Nacional de Promoción Científica y Tecnológica (PICT-2014-2583 & PICT 2016-0508), and Universidad Nacional de La Plata (PPID 2018) partially supported this study.

Conflicts of interest/Competing interests

The authors declare that they have no known competing financial interests or personal relationships that could have appeared to influence the work reported in this paper.

Availability of data and material (data transparency)

All data is available.

Code availability (software application or custom code)

Not applicable

Authors' contributions

Florencia Leis performed investigation. Leonel Long performed formal analysis. Ana Laura Di Virgilio performed conceptualization, funding acquisition, and writing – Review and editing. Pablo M. Arnal performed conceptualization, funding acquisition, and writing – Original Draft & Review and editing.

Animal research

Not applicable.

Consent to Participate

Not applicable.

References

1. Loganathan P, Vigneswaran S, Kandasamy J, Naidu R Defluoridation of drinking water using adsorption processes. J Hazard Mater 2013, 1–19, doi:10.1016/j.jhazmat.2012.12.043
2. He J, Yang Y, Wu Z, Xie C, Zhang K, Kong L, Liu J (2020) Review of fluoride removal from water environment by adsorption. J ofEnvironmental Chem Eng 8:104516. doi:10.1016/j.jece.2020.104516
3. Stöber W, Fink A, Bohn E (1968) Controlled growth of monodisperse silica spheres in the micron size range. J Colloid Interface Sci 26:62–69
4. Xu J, Wu P, Ye EC, Yuan BF, Feng YQ (2016) Metal oxides in sample pretreatment. TrAC - Trends Anal Chem 80:41–56. doi:10.1016/j.trac.2016.02.027
5. Kuang L, Liu Y, Fu D, Zhao Y (2016) FeOOH-Graphene Oxide nanocomposites for fluoride removal from water: acetate mediated nano FeOOH growth and adsorption mechanism. J Colloid Interface Sci 490:259–269. doi:10.1016/j.jcis.2016.11.071
6. Zhang AC, Li Y, Wang T (2017) Synthesis and properties of a high-capacity iron oxide adsorbent for fluoride removal from drinking water. Appl Surf Sci 425:272–281. doi:10.1016/j.apsusc.2017.06.159
7. Chae HS, Kim SD, Piao SH, Choi HJ (2016) Core-shell structured Fe3O4@SiO2 nanoparticles fabricated by sol–gel method and their magnetorheology. Colloid Polym Sci 294:647–655. doi:10.1007/s00396-015-3818-y
8. Alavi Nikje MM, Tamaddoni Moghaddam S, Noruzian M, Farahmand Nejad MA, Shabani K, Haghshenas M, Shakhesi S (2014) Preparation and characterization of flexible polyurethane foam nanocomposites reinforced by magnetic core-shell Fe3O 4@APTS nanoparticles. Colloid Polym Sci 292:627–633. doi:10.1007/s00396-013-3099-2
9. Liu YD, Fang FF, Choi HJ (2011) Core-shell-structured silica-coated magnetic carbonyl iron microbead and its magnetorheology with anti-acidic characteristics. Colloid Polym Sci 289:1295–1298. doi:10.1007/s00396-011-2452-6
10. Zhang JM, Zhai SR, Zhai B, An QD, Tian G (2012) Crucial factors affecting the physicochemical properties of sol-gel produced Fe3O4@SiO2-NH2 core-shell nanomaterials. J Sol-Gel Sci Technol 64:347–357. doi:10.1007/s10971-012-2864-x
11. Zhang J, Liu M, Liu Z, Yang T, He Q, Yang K, Wang H (2017) Studies of malachite green adsorption on covalently functionalized Fe3O4@SiO2–graphene oxides core–shell magnetic microspheres. J Sol-Gel Sci Technol 82:424–431. doi:10.1007/s10971-017-4307-1
12. Samiey B, Cheng CH, Wu J (2014) Organic-inorganic hybrid polymers as adsorbents for removal of heavy metal ions from solutions: A review. Materials (Basel) 7:673–726. doi:10.3390/ma7020673
13. Zhu Y, Jiang FY, Chen K, Kang F, Tang ZK (2013) Modified reverse microemulsion synthesis for iron oxide/silica core-shell colloidal particles. J Sol-Gel Sci Technol 66:180–186. doi:10.1007/s10971-013-2985-x
14. Meng SC, Wang H, Qing M, Qiu CW, Yang Y, Li YW (2015) Preparation and characterization of SiO2@Fe2O3 core-shell catalysts. J Fuel Chem Technol 43:692–700. doi:10.1016/s1872-5813(15)30020-7
15. Regulatory Affairs TFS Safety Data Sheet: Iron(III) acetylacetonate Available online: https://www.fishersci.com/store/msds?partNumber=AC119130010&productDescription=IRON%28III%29+ACETYLACETONAT+1KG&vendorId=VN00032119&countryCode=US&language=en (accessed on Oct 19, 2020)
16. Anastas PT, Warner JC *Green Chemistry Theory and Practice*; Oxford University Press: New York (EEUU); ISBN 0-19-850698-8

17. Safety data sheet: Iron(III) nitrate nonahydrate Available online: www.carlroth.com/downloads/sdb/en/5/SDB_5632_AU_EN.pdf (accessed on Oct 19, 2020)
18. Arnal PM, Weidenthaler C, Schüth F (2006) Highly monodisperse zirconia-coated silica spheres and zirconia/ silica hollow spheres with remarkable textural properties. Chem Mater 18:2733–2739. doi:10.1021/cm052580a
19. Montgomery CD *Design and analysis of experiments*; 6th ed.; John Wiley & Sons Inc, 2005; ISBN 0-471-48735-X
20. ASTM International ASTM D1179-99, Standard Test Methods for Fluoride Ion in Water., doi:10.1520/D1179-99
21. Montgomery DC *Applied Statistics and Probability for Engineers Third Edition*; 3rd ed.; John Wiley & Sons Inc, 2003; ISBN 0471204544
22. Rahman MM, Govindarajulu Z (1997) A modification of the test of Shapiro and Wilk for normality. J Appl Stat 24:219–236. doi:10.1080/02664769723828
23. Di Rienzo JA, Casanoves F, Balzarini M, Gonzalez L, Tablada M, Robledo CW, InfoStat. Software estadístico. Versión estudiantil 2014
24. Grubbs FE (1950) Sample Criteria for Testing Outlying Observations. Ann Math Stat 21:27–58. doi:10.1214/aoms/1177729885
25. Wright JD, Sommerdijk AJM *Sol-Gel Materials Chemistry and Applications*; Phillips, S.., Ed.; Taylor & Francis: Liverpool (UK), 2001; Vol. 4; ISBN 90-5699-326-7
26. Keller A, Wlokas I, Kohns M, Hasse H (2020) Thermophysical Properties of Solutions of Iron(III) Nitrate-Nonahydrate in Mixtures of Ethanol and Water. J Chem Eng Data 65:3519–3527. doi:10.1021/acs.jced.0c00105
27. Ledda M, Fioretti D, Lolli MG, Papi M, Di Gioia C, Carletti R, Ciasca G, Foglia S, Palmieri V, Marchese R et al (2020) Biocompatibility assessment of sub-5 nm silica-coated superparamagnetic iron oxide nanoparticles in human stem cells and in mice for potential application in nanomedicine. Nanoscale 12:1759–1778. doi:10.1039/c9nr09683c
28. Williams LJ, Zosky GR (2019) The Inflammatory Effect of Iron Oxide and Silica Particles on Lung Epithelial Cells. Lung 197:199–207. doi:10.1007/s00408-019-00200-z
29. Andujar P, Simon-Deckers A, Galateau-Sallé F, Fayard B, Beaune G, Clin B, Billon-Galland MA, Durupthy O, Pairon JC, Doucet J et al (2014) Role of metal oxide nanoparticles in histopathological changes observed in the lung of welders. Part Fibre Toxicol 11:1–13. doi:10.1186/1743-8977-11-23
30. Rushton L (2007) Chronic obstructive pulmonary disease and occupational exposure to silica. Rev Environ Health 22:255–272. doi:10.1515/REVEH.2007.22.4.255
31. Iler RK *The chemistry of silica. Solubility, polymerization, colloid and surface properties, and biochemistry.*; John Wiley & Sons: New York (EEUU), 1979; ISBN 0-471-02404-X
32. Mukherjee S, Halder G (2018) A review on the sorptive elimination of fluoride from contaminated wastewater. J Environ Chem Eng 6:1257–1270. doi:10.1016/j.jece.2018.01.046
33. Habuda-Stanić M, Ravančić M, Flanagan AA (2014) Review on Adsorption of Fluoride from Aqueous Solution. Materials (Basel) 7:6317–6366. doi:10.3390/ma7096317
34. Vinati A, Mahanty B, Behera SK (2015) Clay and clay minerals for fluoride removal from water: A state-of-the-art review. Appl Clay Sci 114:340–348. doi:10.1016/j.clay.2015.06.013
35. Di Virgilio AL, Maisuls I, Kleitz F, Arnal PM (2013) A new synthesis pathway for colloidal silica spheres coated with crystalline titanium oxide and its comparative cyto- and genotoxic study with titanium oxide nanoparticles in rat osteosarcoma (UMR106) cells. J Colloid Interface Sci 394:147–156. doi:10.1016/j.jcis.2012.11.005

Figures

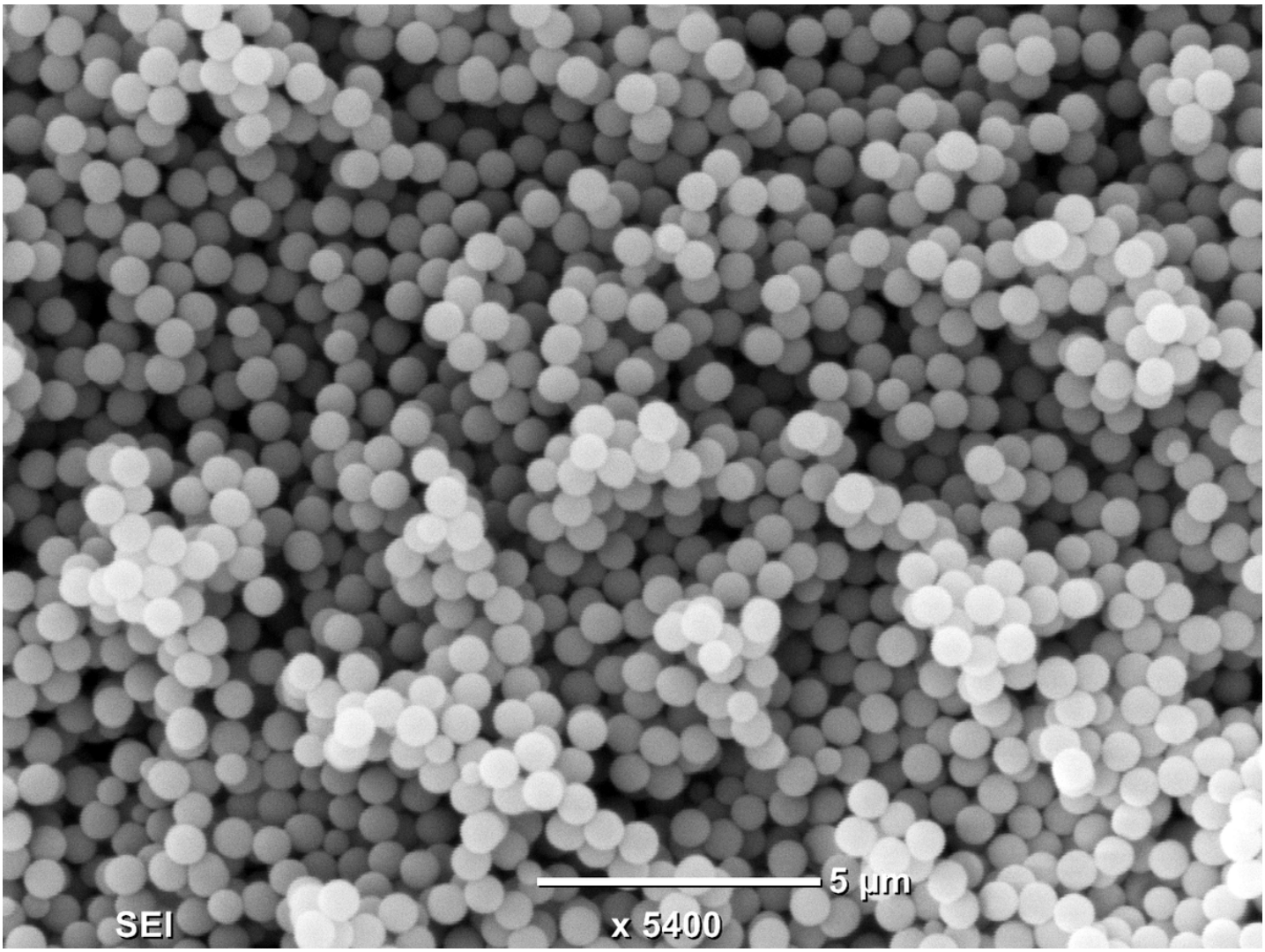

Figure 1

SEM images of SiO2 spheres after treatment with Fe(NO3)3 in absolute ethanol. With GIMP Software, we adjusted the brightness of the image to -32 and contrast to +35.

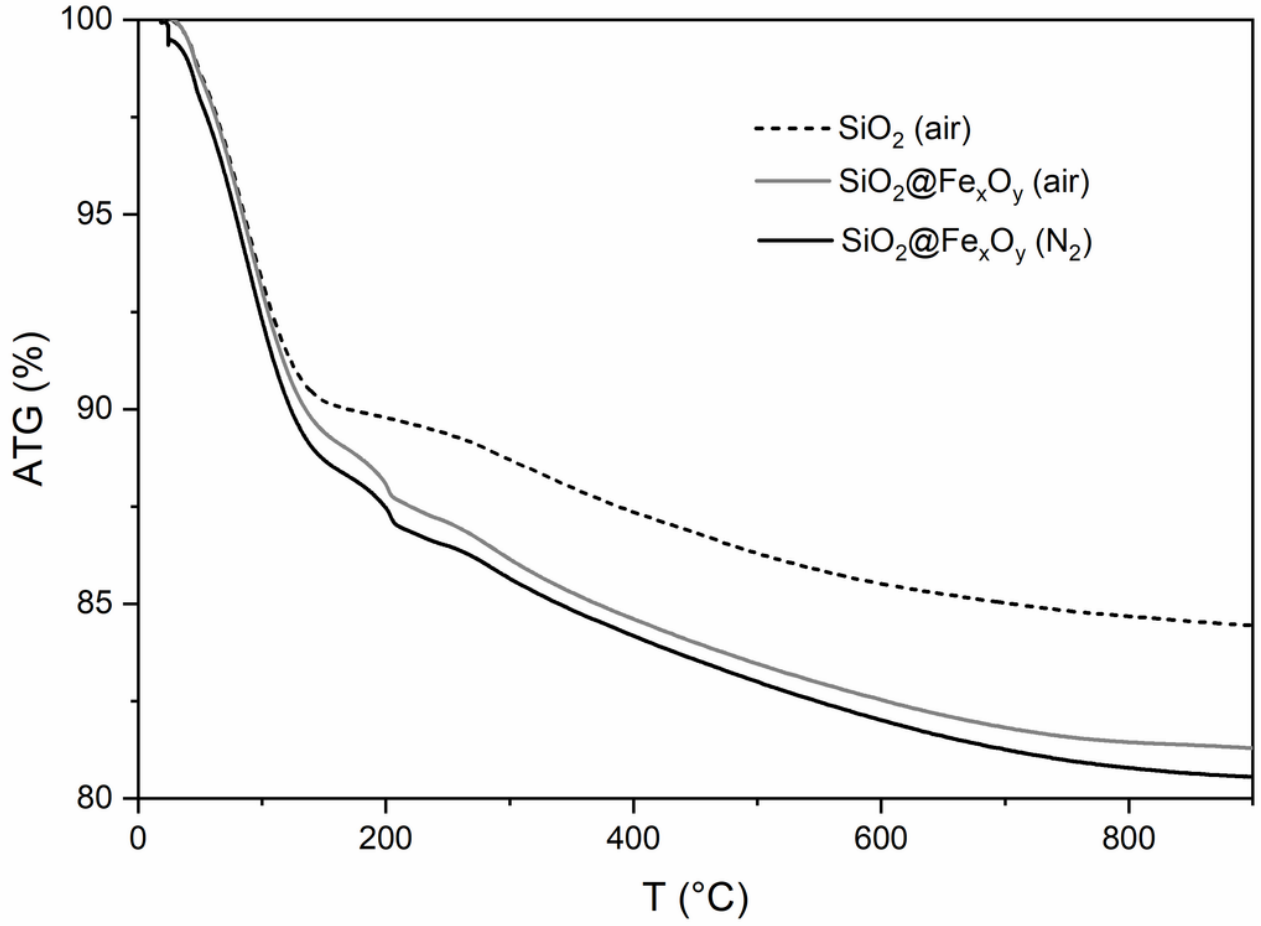

Figure 2

Thermal gravimetric analyses of SiO2 spheres before and after treatment with Fe(NO3)3 in absolute ethanol. In the latter, either under air or N2.

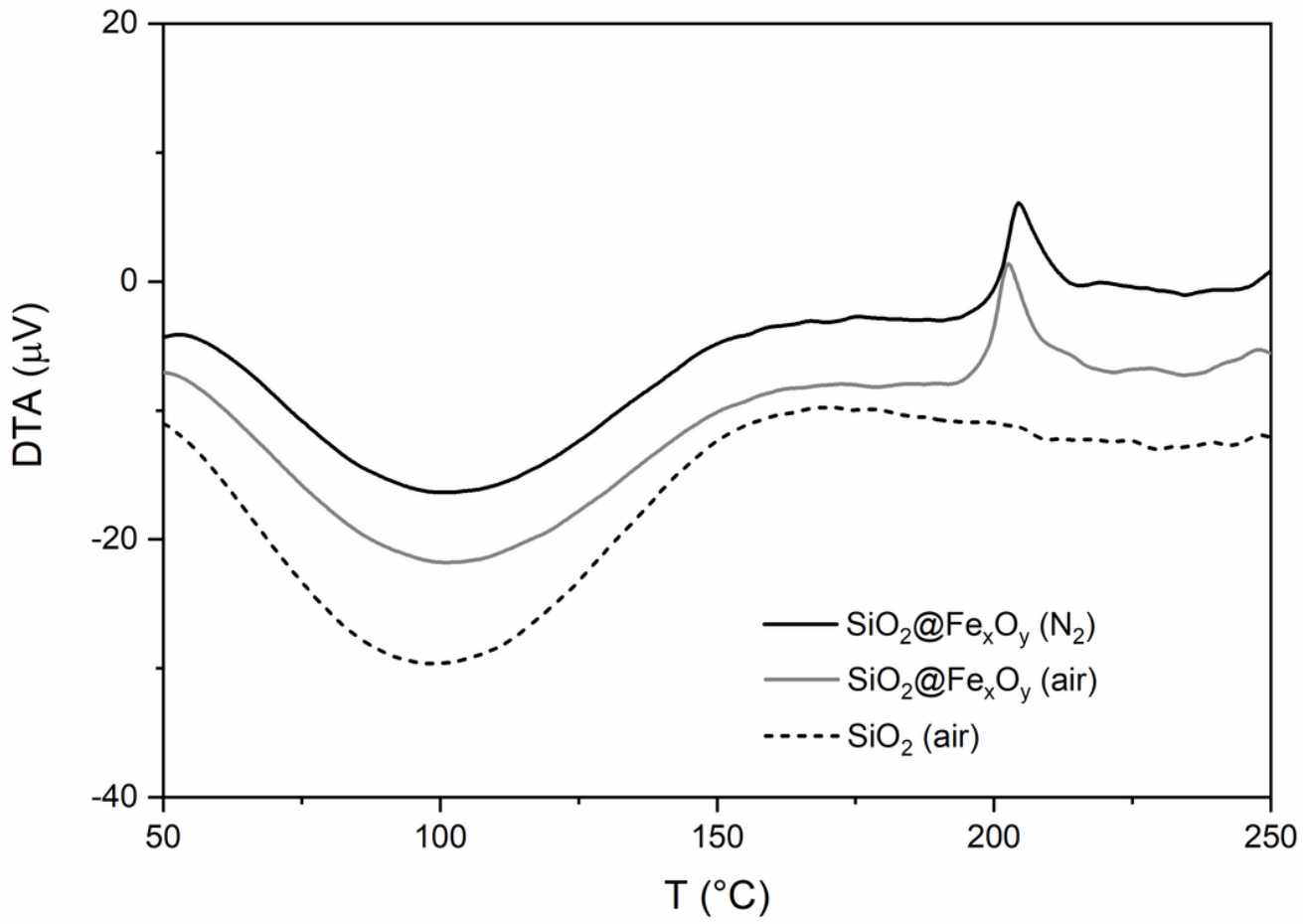

Figure 3

Differential thermal analyses of SiO2 spheres before (dashed line) and after treatment with Fe(NO3)3 in ethanol either under air (light gray line) or N2 (black line). The endothermic signal below originated in the evaporation of water. The exothermic process occurred only in the material after exposure to iron nitrate.

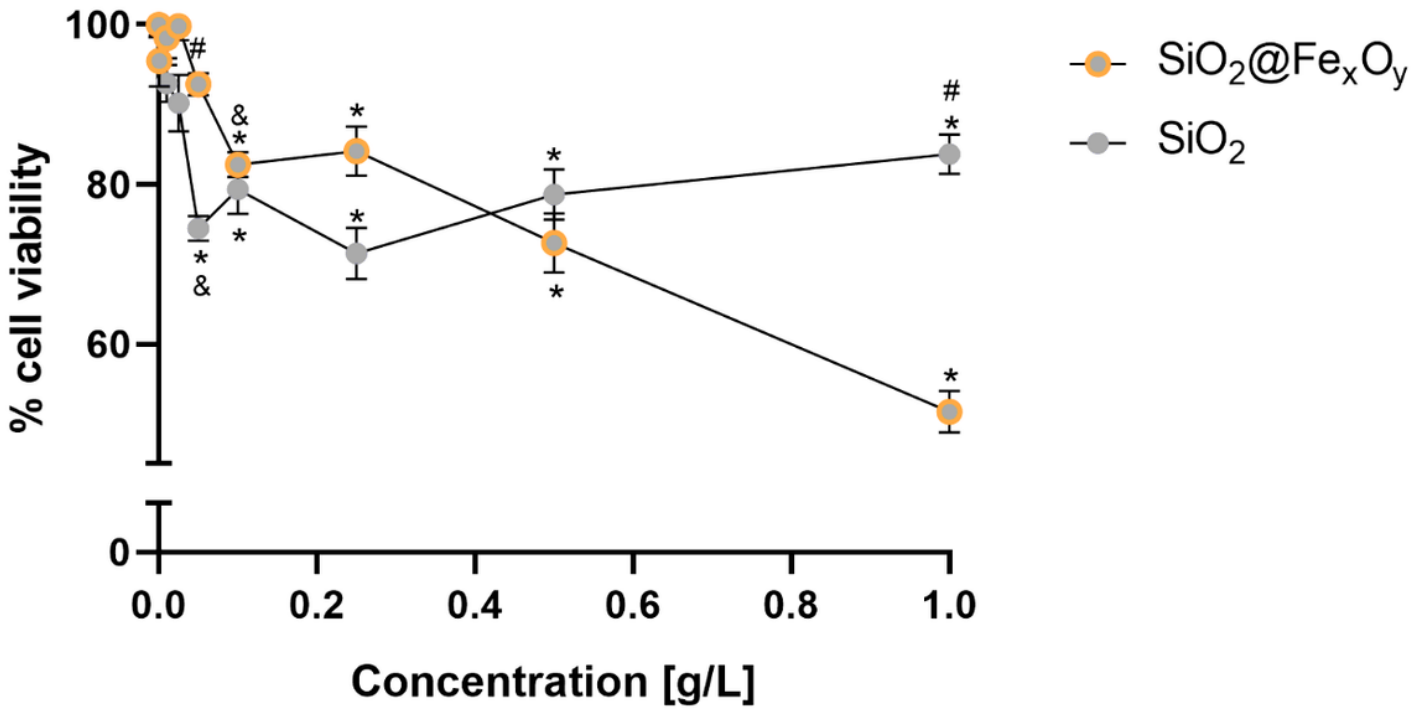

Figure 4

Effect of SiO2@FexOy particles on cell viability in A549 cells. Asterisks represent statistically significant difference with solvent control (* p<0.001) (n=12)), # statistically significant difference between particles (p<0.001), & statistically significant difference in relation with the previous concentration (p<0.001).

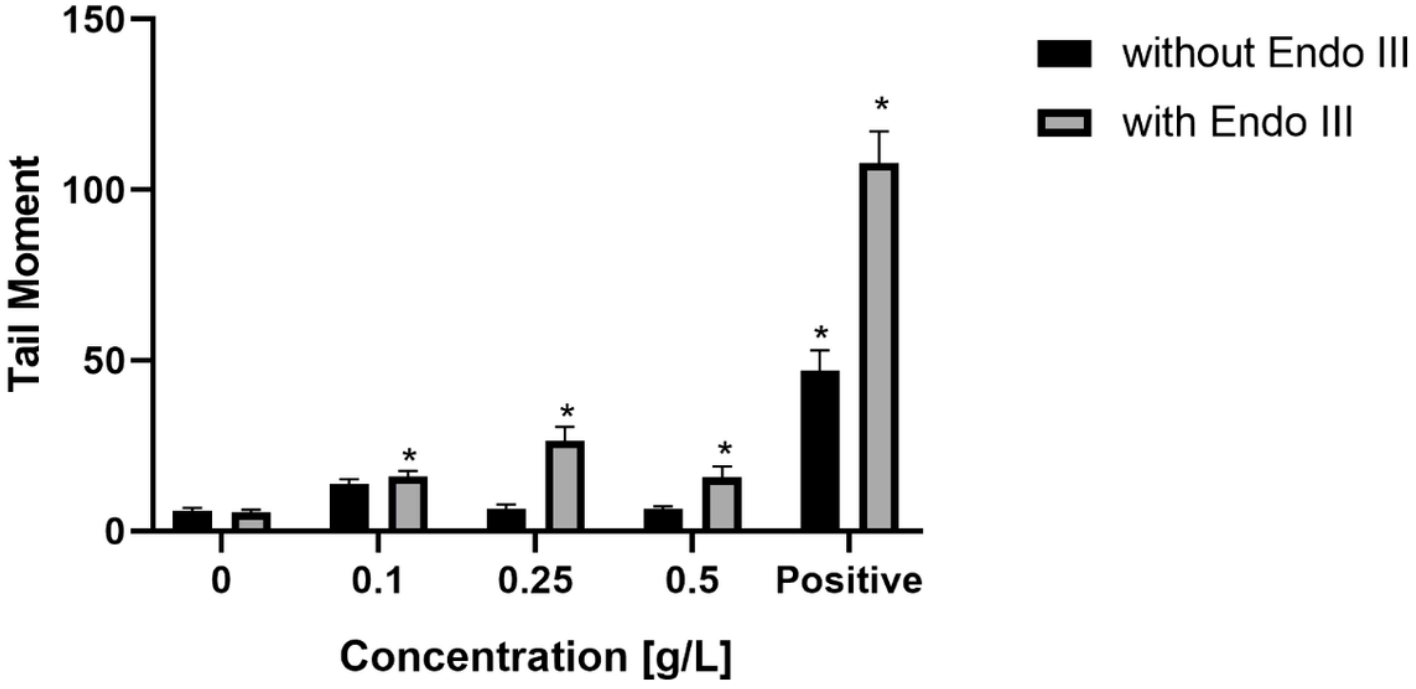

Figure 5

The Comet assay studied DNA damage in A549 cells treated with SiO2@FexOy particles during 24 h. Asterisks (*) represent a statistically significant difference with control cells (p<0.01).

Supplementary Files

This is a list of supplementary files associated with this preprint. Click to download.

- Scheme1.png
- SupplementaryInformation.docx